HAL open science

# Spherical Phaseless Antenna Measurements Experimental Validation of a Two-Antenna-Positions Procedure

Nicolas Mezieres, Laurent Le Coq, Benjamin Fuchs

▶ **To cite this version:**

Nicolas Mezieres, Laurent Le Coq, Benjamin Fuchs. Spherical Phaseless Antenna Measurements Experimental Validation of a Two-Antenna-Positions Procedure. IEEE Antennas and Wireless Propagation Letters, 2022, 21 (4), pp.813-817. 10.1109/LAWP.2022.3149304 . hal-03657159

**HAL Id: hal-03657159**

**https://hal.science/hal-03657159v1**

Submitted on 16 Jun 2022

**HAL** is a multi-disciplinary open access archive for the deposit and dissemination of scientific research documents, whether they are published or not. The documents may come from teaching and research institutions in France or abroad, or from public or private research centers.

L'archive ouverte pluridisciplinaire **HAL**, est destinée au dépôt et à la diffusion de documents scientifiques de niveau recherche, publiés ou non, émanant des établissements d'enseignement et de recherche français ou étrangers, des laboratoires publics ou privés.

This article has been accepted for publication in a future issue of this journal, but has not been fully edited. Content may change prior to final publication. Citation information: DOI 10.1109/LAWP.2022.3149304, IEEE Antennas and Wireless Propagation Letters



# Spherical Phaseless Antenna Measurements Experimental Validation of a Two Antenna Positions Procedure

Nicolas Mézières, Laurent Le Coq, and Benjamin Fuchs, *Senior Member, IEEE*

***Abstract*—The phaseless characterization of antennas enables to reduce the cost and to ease the measurement of radiating systems, especially at high frequencies. The complex near field is retrieved from the acquisition of the antenna radiated field magnitude only thanks to appropriate phase retrieval algorithms. Thus, a two scan approach combined to a Gerchberg-Saxton algorithm has proven to lead to accurate phase retrievals. However, instead of measuring the field on two spherical surfaces of different radii as conventionally performed, we propose to measure the magnitude of the field on a single sphere but for two antenna positions. This new strategy is easier to implement in a number of measurement setups. Numerical and experimental validations in a commercial, arch-based, measurement system are shown and discussed.**

***Index Terms*—Antenna measurements, near field, phaseless measurement, phase retrieval, spherical waves.**

## I. Introduction

SPHERICAL Near-Field (NF) antenna measurement is a standard, accurate and mature technique for antenna characterization [1]–[3]. However, the phase of the radiated field might be cumbersome and costly to be acquired accurately. Phaseless, or magnitude-only, antenna measurements are an attractive solution to relax the demanding constraints (probe positioning, cable bending, temperature stability, ...) required to ensure reliable phase measurements and consequently reduce the cost of such characterization. The price to pay is the increased number of required sampling points and the significant and notorious numerical difficulties of phase retrieval problems.

In phaseless NF antenna measurements, the complex radiation pattern is retrieved from magnitude only measurements. Among the categories of phaseless antenna measurements, the two scans technique is arguably the most commonly used as well explained in [4]. The magnitude of the field radiated by the Antenna Under Test (AUT) is measured over two surfaces that must be sufficiently separated in order to mitigate the otherwise inevitable ambiguities arising in phase retrieval problems. This strategy has proven to provide excellent results in the case of phaseless spherical NF antenna measurements, as recently investigated thoroughly in [5]. The magnitude of the field is sampled on two concentric spheres and the influence of their radii is investigated. The Gerchberg-Saxton (GS) algorithm [6] is used to solve the phase retrieval problem and reconstruct the complex NF over one sphere in order to derive the Far Field (FF) radiated by the AUT.

Manuscript received 12, 2021; revised 01, 2022.

This work was carried out in the frame of a CNES and LNE grant and is supported in part by the European Union through the European Regional Development Fund (ERDF), and by the french region of Brittany, Ministry of Higher Education and Research, Rennes Métropole and Conseil Départemental 35, through the CPER Project SOPHIE / & STIC Ondes.

N. Mézières and L. Le Coq are with IETR, Rennes, France (e-mail: nicolas.mezieres@univ-rennes1. fr), and B. Fuchs is the Federal Office of Communications, Switzerland.

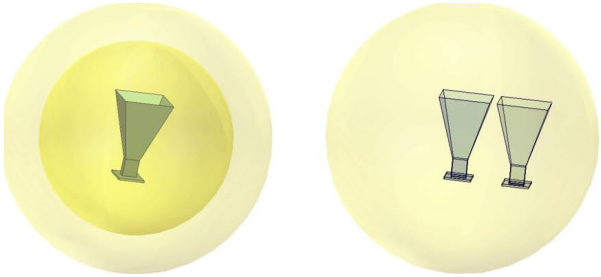

Fig. 1. Illustration of two configurations of phaseless spherical NF antenna measurements. The intensity of the NF is measured (left) on two concentric spheres and (right) on a single sphere for two antenna positions.

Among the many recent phase retrieval algorithms, including convex methods [7], [8] and non-convex techniques [9], the pioneer alternating projection algorithm of GS, turns out to perform very well under appropriate conditions of field sampling (e.g. sampling density and sphere radii), as shown in [5].

This letter proposes and validates experimentally a different phaseless spherical NF antenna measurement procedure, where the two scans are performed over a single measurement sphere for two positions of the antenna. The shift of the AUT inside the measurement sphere enables to generate the two independent magnitude measurement datasets required in any phaseless measurement procedure. This scenario, first mentioned in [10], has been recently numerically investigated in [11]. An experimental validation of such a phaseless antenna measurement is shown and discussed here for the first time to our best knowledge. Moreover, the present algorithm is more efficient as it avoids working in the FF domain in order to translate the field. Consequently, our approach does not requires a higher truncation order for the modal expansion of the shifted antenna. Also the proposed strategy is not restricted to constant angular step distributions.

The phaseless measurement over a single sphere for two antenna positions is easier to implement in a number of relevant measurement setups, such as arch-based systems. The usual two scan configuration for spherical phaseless measurement and the new one investigated in this letter are represented in Fig. 1. The link between the measurement settings (field sampling, antenna positions) and the accuracy of the phase retrieval is investigated to better understand the conditions of a successful phaseless measurement procedure.

The letter is organized as follows. In Section II, the spherical wave expansion and the standard two scan technique are recalled, the proposed two antenna position for phaseless pro-

ACCEPTED MANUSCRIPT - CLEAN COPY

This article has been accepted for publication in a future issue of this journal, but has not been fully edited. Content may change prior to final publication. Citation information: DOI 10.1109/LAWP.2022.3149304, IEEE Antennas and Wireless Propagation Letters



cedure is also described. The proposed approach is validated on a numerical example in Section III with a discussion on the phase retrieval accuracy and experimental cases are shown in Sections IV. Finally, conclusions are drawn in Section V.

## II. Phaseless Antenna Spherical Measurement

### A. Spherical Wave Expansion

The electric field $\mathbf{E}$ radiated from sources can be expanded outside the minimal sphere using Spherical Waves (SW) $\mathbf{F}_{smn}$ as follows [1]

$$\mathbf{E}(r,\theta,\varphi) = \frac{k}{\sqrt{\eta}} \sum_{smn} Q_{smn} \mathbf{F}_{smn}(r,\theta,\varphi) \tag{1}$$

where $k$ is the wavenumber, $\eta$ the admittance of the propagation medium and $(r,\theta,\varphi)$ the spherical coordinates. The quantities $Q_{smn}$ are the complex spherical coefficients to be determined. The SW are indexed by $s \in \{1,2\}$ the propagation mode, $n$ the degree and $|m| \leq n$ the order. The series (1) is truncated to $n \leq N$ according to the rule $N = \lfloor ka \rfloor + n_1$ where $a$ is radius of the minimal sphere, $\lfloor x \rfloor$ the floor function and $n_1$ an integer [1], often fixed to 10 [12].

If the electric field radiated by the AUT is measured at $M$ sampling positions over a sphere of radius $R$, the SW expansion of the field (1) can be rewritten as a linear system of equations

$$\mathbf{y} = \mathbf{A}\mathbf{x} \tag{2}$$

where the vector $\mathbf{y}$ of size $2M$ gathers the complex measured field (two polarizations), $\mathbf{A}$ is the matrix containing the discretization of the SW, $\mathbf{F}_{smn}$, at the sampling positions and $\mathbf{x}$ stores the spherical coefficients $Q_{smn}$. The SW matrix $\mathbf{A}$ is modified according to the transmission formula for NF measurements to compensate for the probe radiation pattern as detailed from p. 61 in [1].

### B. Phase Retrieval Formulation and Resolution Methods

Only the magnitude of the field i.e. $|\mathbf{y}|$, is measured. However the phase is necessary to perform the Near-Field to Far-Field (NF2FF) transformation. Therefore a phase retrieval procedure, a GS like algorithm, is considered in this letter.

It has also been shown that sampling strategies have an influence on the accuracy achieved by phaseless measurements [13]. More specifically, uniformly distributed sampling are more efficient. Consequently, the igloo sampling [14], providing such property, is used throughout this letter. A first accuracy assessment based on the orthogonality of the SW for each position of the AUT is also demonstrated.

### C. Gerchberg-Saxton for two Spheres

The standard GS algorithm for spherical antenna measurements propagates the retrieved complex field back and forth between the two spheres of different radii until convergence. Indeed, the fields over each sphere must share the same spherical coefficients $Q_{smn}$. The coefficients identified over one sphere are used to perform a back or forward propagation to the other one. At each propagation to the other measurement sphere, the magnitude is replaced by the measured one and the process goes on until some stopping criterion is satisfied [5].

### D. Gerchberg-Saxton for two Antenna Positions

The two concentric sphere procedure can be easily adapted to a single measurement sphere for two antenna positions provided that the expansion of the radiated field leads to the same spherical coefficients. This is achieved by an analytical transformation of the SW basis [1]. In particular, the radiated field of a shifted antenna, as in Fig. 1, has exactly the same spectrum as before if the shift is also applied to the SW basis. It can also be interpreted as measurements over two non-concentric spheres in the same AUT coordinate system.

Let $\mathbf{y}$, $\mathbf{y}_T$ the measured fields for the antenna default and shifted away positions respectively, $\mathbf{A}$ the SW matrix as in (2) and $\mathbf{A}_T$ the matrix containing the translated SW. Therefore the following equations hold: $\mathbf{A}\mathbf{x} = \mathbf{y}, \mathbf{A}_T\mathbf{x} = \mathbf{y}_T$. The modified GS algorithm for two antenna positions is given in Algorithm 1. As indicated in the introduction, a similar algorithm was given in [11]. However, the present version avoids the FF propagation step along the reference point method and uses a matrix-vector formulation approach (2).

**Algorithm 1** Modified Gerchberg-Saxton for phaseless measurements with two AUT positions

**Require:** $|\mathbf{y}|, |\mathbf{y}_T|$ the measured magnitude and $\mathbf{A}, \mathbf{A}_T$ the SW matrices for the two AUT positions, $\phi^{(0)}$ a starting phase guess.

**Initialization**
$\widetilde{\mathbf{y}} \leftarrow |\mathbf{y}| e^{i\phi^{(0)}}$
**while** Stopping criterion not met **do**
  $\mathbf{x} \leftarrow \widetilde{\mathbf{A}}^{+}\widetilde{\mathbf{y}}$ #Solving for the coefficients
  $\widetilde{\mathbf{y}}_T \leftarrow \mathbf{A}_T\mathbf{x}$ #Apply translation
  $\boldsymbol{\phi}_T \leftarrow \text{Phase}(\widetilde{\mathbf{y}}_T)$ #Store the retrieved phase
  $\widetilde{\mathbf{y}}_T \leftarrow |\mathbf{y}_T| e^{i\boldsymbol{\phi}_T}$ #Magnitude correction
  $\mathbf{x} \leftarrow \widetilde{\mathbf{A}}_T^{+}\widetilde{\mathbf{y}}_T$ #Solving for the coefficients
  $\widetilde{\mathbf{y}} \leftarrow \mathbf{A}\mathbf{x}$ #Apply translation
  $\boldsymbol{\phi} \leftarrow \text{Phase}(\widetilde{\mathbf{y}})$ #Store the retrieved phase
  $\widetilde{\mathbf{y}} \leftarrow |\mathbf{y}| e^{i\boldsymbol{\phi}}$ #Magnitude correction
**return** $\mathbf{x}$ #Spherical coefficients.

In this paper, a constant phase initialization, $\phi^{(0)} = 0$ is used, as in [5]. This simple start is good enough to show the feasibility of our phaseless configuration but other starting points should be considered to improve the convergence. The resolutions of the linear systems are performed in a regularized least square sense. It boils down to a multiplication of the data vector by the pseudo-inverse of the low-rank approximation of the SW matrices, $\widetilde{\mathbf{A}}^{+}$ and $\widetilde{\mathbf{A}}_T^{+}$. It enables a computationally fast and efficient algorithm once the matrices have been computed offline.

## III. Numerical Validations

### A. Reconstruction Metric

The success of the phaseless characterization is evaluated by comparing the retrieved FF in $\widetilde{\mathbf{y}}$ to the reference one, $\mathbf{y}$. This comparison is achieved point-wise using the error signal defined by

$$\text{Error}(\mathbf{y}, \widetilde{\mathbf{y}}) = \frac{||\mathbf{y}| - |\widetilde{\mathbf{y}}||}{\max_i |\mathbf{y}_i|}. \tag{3}$$

ACCEPTED MANUSCRIPT - CLEAN COPY

This article has been accepted for publication in a future issue of this journal, but has not been fully edited. Content may change prior to final publication. Citation information: DOI 10.1109/LAWP.2022.3149304, IEEE Antennas and Wireless Propagation Letters



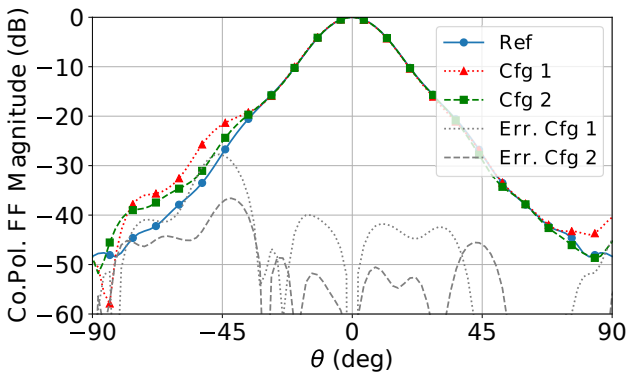


Fig. 2. Simulated horn: FF reconstruction of the field from the phaseless spherical NF measurements in the main polarization plane.

The mean of this error signal defines the Equivalent Noise Level (ENL) and both are given on a dB scale in the sequel. In this letter, only the FF magnitudes are compared because they provide a simple indicator of a coherent retrieved phase from NF measurements.

### B. Simulated Horn Antenna at 10 GHz

Let us consider the numerical model of the standard gain horn in X-band shown in Fig. 4.(a). The field is derived where needed by reference spherical coefficients coming from a very dense simulation data set. The two antenna positions procedure is tested for two configurations, denoted as Cfg. 1 and Cfg. 2. A shift on the $z$ axis is applied to provide the two positions in both cases. These translations have a length of $30\,\mathrm{mm}$ for Cfg. 1 and $60\,\mathrm{mm}$ for Cfg. 2 (1 and $2\lambda$). The NF samplings are generated on a sphere of $260\,\mathrm{mm}$ with respect to the origin (20 % of the Rayleigh FF distance) with 2744 samples for 1248 unknowns, corresponding to a truncation order of the SW expansion of $N = 24$. The reconstruction of the FF in the co-polarization plane is shown in Fig. 2. The ENL for reconstructions from Cfg. 1 and Cfg. 2 on the whole sphere are $-41.7\,\mathrm{dB}$ and $-43.8\,\mathrm{dB}$ respectively. It demonstrates the numerical reliability of the proposed phase retrieval strategy and algorithm.

### C. Correlation and Phase Retrieval Accuracy

Phase ambiguities emerge more often when the measurement matrix $\mathbf{A}$ possesses redundancies, as showcased in [13]. Consequently, the correlation between the modes stored in matrices $\mathbf{A}$ and $\mathbf{A}_T$ provides an indicator of the expected phase retrieval accuracy. The correlation between two discretized modes is the modulus of complex inner product between the two corresponding normalized columns in the SW matrices. The higher the redundancy, the higher the correlation. The histograms of correlations between the SW matrices for Cfg. 1 and Cfg. 2 are shown in Fig. 3. As expected, the Cfg. 2, leading to better FF reconstruction, uses matrices showing less redundancies. Numerous tests for various shift distances on the $z$-axis have been led to confirm this behaviour and are not shown here for conciseness and readability. For a given measurement setup, this histogram provides a comparison tool between two antenna position configuration for phaseless measurement.

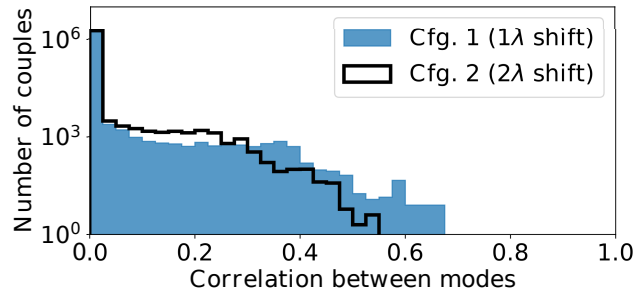


Fig. 3. Correlation histograms between the columns of the SW matrices for two antenna shift configurations (1 and 2 $\lambda$). The histogram displays the number of spherical mode couples distribution with respect to their correlations.

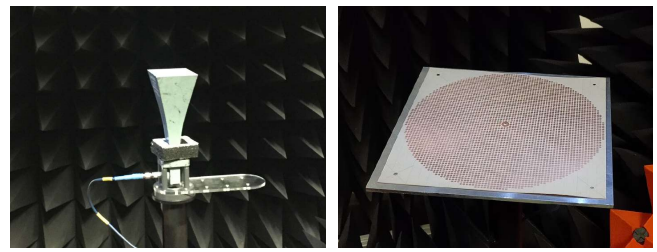

(a) Horn (b) Metasurface [16]

Fig. 4. Pictures of the antennas measured in the MVG Starlab for the experimental validations of the phaseless characterization procedure.

## IV. Experimental Validations

Two NF measurements, performed in the MVG Starlab [15] of the IETR-INSA, are presented; a standard gain horn at $10\,\mathrm{GHz}$ and a metasurface at $17\,\mathrm{GHz}$ [16], both shown in Fig. 4. The spherical coefficients returned by the MVG software are used to construct the phaseless NF at the radius of the probes and also to compute the reference FF.

### A. Horn Antenna at 10 GHz

The NF data are made of 3088 measurements along an igloo sampling for 1350 unknowns (truncation order $N = 25$, sampling ratio $\approx 2.3$ per AUT position). The applied shift between the two positions is of $3\lambda = 9\,\mathrm{cm}$. FF reconstructions of the co and cross-polarizations in the main cutting plane are shown in Fig. 5. The ENL of the reconstruction over the whole sphere is $-39.9\,\mathrm{dB}$.

### B. Metasurface Antenna at 17 GHz

The NF data are made of 13876 measurements along an igloo sampling for 6493 unknowns (truncation order $N = 56$, sampling ratio $\approx 2.2$ per AUT position). The applied shift is of $2\lambda \approx 3.5\,\mathrm{cm}$. FF reconstructions of $E_\theta$ and $E_\varphi$ polarizations in the main cutting plane are shown in Fig. 6. The ENL of the reconstruction over the whole sphere is $-34.9\,\mathrm{dB}$. This quite high value is explained by a higher magnitude mean of the radiation pattern itself, as hinted by the cuts in Fig. 6.

ACCEPTED MANUSCRIPT - CLEAN COPY

This article has been accepted for publication in a future issue of this journal, but has not been fully edited. Content may change prior to final publication. Citation information: DOI 10.1109/LAWP.2022.3149304, IEEE Antennas and Wireless Propagation Letters



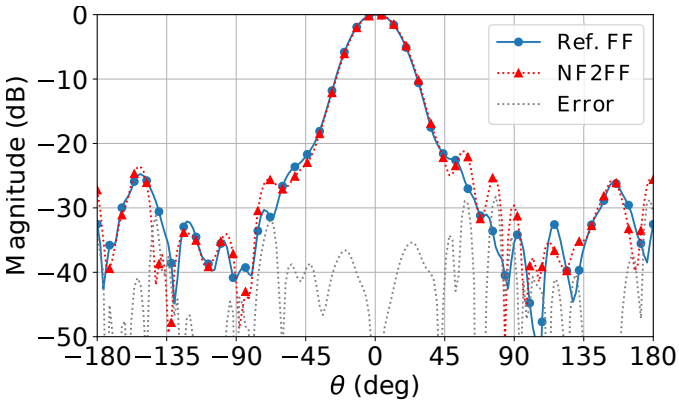


(a) Co-polarization

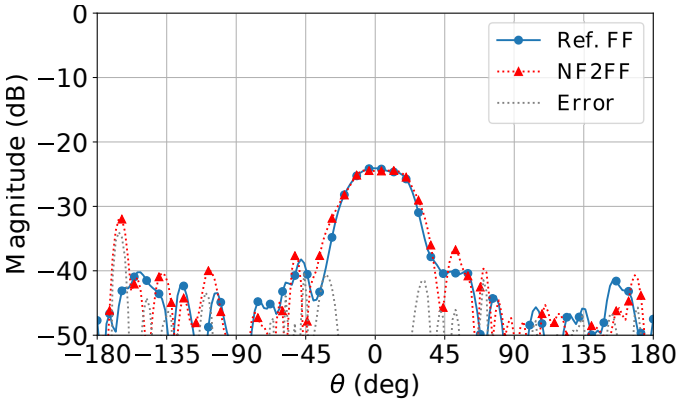


(b) Cross-polarization

Fig. 5. Measured horn: FF reconstruction of the field from the phaseless spherical NF measurements.

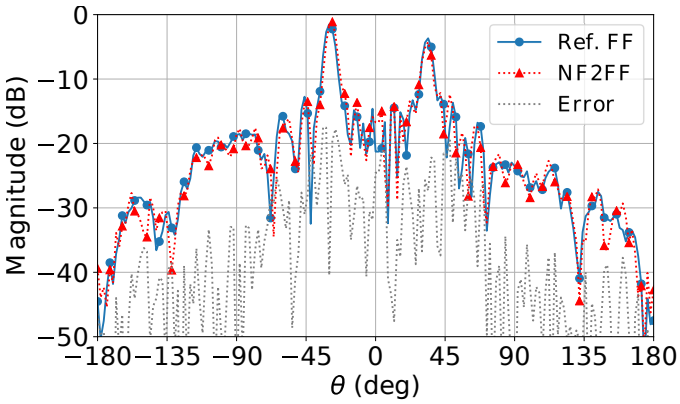


(a) $E_\theta$

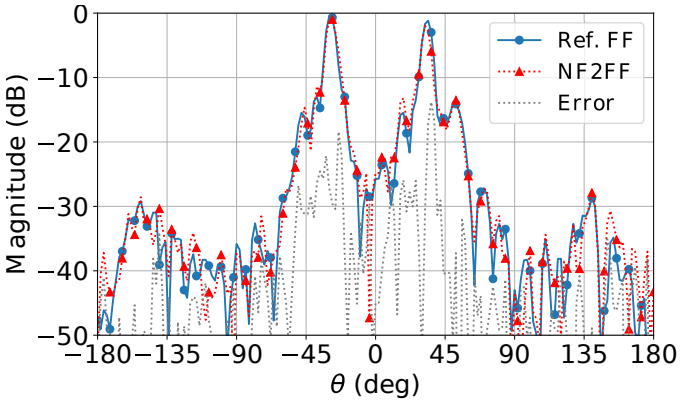


(b) $E_\varphi$

Fig. 6. Measured metasurface: FF reconstruction of the field from the phaseless spherical NF measurements.

## V. Conclusion

A phaseless spherical antenna measurement strategy has been investigated and experimentally validated. The approach consists in measuring the radiated field magnitude on a single near field sphere for two antenna positions. This phaseless measurement configuration is suitable for arch-based measurement systems and is complementary to the commonly used two sphere approach. In addition, the measurement settings of this two antenna position approach to ensure a proper phase retrieval and mitigate the phase ambiguities have been investigated from the computation of the correlation between the two measurement matrices. These first promising experimental results show that the proposed antenna phaseless measurement procedure could be an interesting alternative to the widely spread and accurate two sphere approach.

## Acknowledgment

The authors thank Jérôme Sol for his help in measuring the antennas.

## References

[1] J. Hald, J. Hansen, F. Jensen, and F. Larsen, *Spherical Near Field Antenna Measurements*. Peter Peregrinus, 1988.

[2] "IEEE recommended practice for near-field antenna measurements," *IEEE Std 1720-2012*, pp. 1–102, 2012.

[3] O. Breinbjerg, "Spherical near-field antenna measurements — the most accurate antenna measurement technique," in *APSURSI*, 2016.

[4] O. Breinbjerg and J. Fernandez Alvarez, "Phaseless near-field antenna measurement techniques – an overview," in *AMTA*, United States, 2016.

[5] F. Rodriguez Varela, J. Fernandez Álvarez, G. Belén Iragüen, M. Sierra Castañer, and O. Breinbjerg, "Numerical and experimental investigation of phaseless spherical near-field antenna measurements," *IEEE Trans. on Antennas and Prop.*, 2021.

[6] R. W. Gerchberg and W. O. Saxton, "A practical algorithm for the determination of phase from image and diffraction plane pictures," *Optik*, vol. 35, no. 10, pp. 237–246, 1972.

[7] E. J. Candès, Y. C. Eldar, T. Strohmer, and V. Voroninski, "Phase retrieval via matrix completion," *SIAM Review*, vol. 57, no. 2, 2015.

[8] T. Goldstein and C. Studer, "Phasemax: Convex phase retrieval via basis pursuit," *IEEE Trans. on Information Theory*, vol. 64, no. 4, 2018.

[9] E. J. Candès, X. Li, and M. Soltanolkotabi, "Phase retrieval via wirtinger flow: Theory and algorithms," *IEEE Trans. Inf. Theory*, no. 4, 2015.

[10] O. Breinbjerg and J. F. Álvarez, "Mathematical formulation of phase retrieval for phaseless spherical near-field antenna measurements with probe correction," in *URSI EMTS*, 2019.

[11] J. Fernandez Alvarez, M. Mattes, and O. Breinbjerg, "Phase retrieval for spherical near-field measurements using two antenna positions," in *AMTA, Florida*, 2021.

[12] F. Jensen and A. Frandsen, "On the number of modes in spherical wave expansions," in *AMTA 2004*, 10.

[13] A. Bangun, A. Behboodi, and R. Mathar, "Signal recovery from phaseless measurements of spherical harmonics expansion," in *2019 27th European Signal Processing Conference (EUSIPCO)*, 2019, pp. 1–5.

[14] B. Fuchs, L. Le Coq, S. Rondineau, and M. Migliore, "Fast antenna far field characterization via sparse spherical harmonic expansion," *IEEE Trans. on Antennas and Propag.*, vol. 65, no. 10, Oct. 2017.

[15] "Starlab 650MHz-18GHz," MVG, 2020, available at www.mvg-world.com/fr/products/antenna-measurement/multi-probe-systems/starlab.

[16] D. Gonzalez-Ovejero, G. Minatti, E. Martini, G. Chattopadhyay, and S. Maci, "Shared aperture metasurface antennas for multibeam patterns," in *EUCAP*, 2017, pp. 3332–3335.

ACCEPTED MANUSCRIPT - CLEAN COPY